XLVI CILAMCE
VITÓRIA - ES - BRAZIL - 2025
XLVI IBERO-LATIN AMERICAN CONGRESS ON COMPUTATIONAL METHODS IN ENGENEERING

Nonlinear static analysis of guyed towers considering unilateral contact of the guys

Victorino Victor Matias[1], Frederico Martins Alves da Silva[1], Arthur Álax Araújo de Albuquerque[1]

[1]*School of Civil and Environmental Engineering - EECA, Federal University of Goiás - UFG*
Avenida Universitária, no. 1488, 74605-220, Goiânia, Brasil
victorino_matias@discente.ufg.br, silvafma@ufg.br, arthuralax@ufg.br

Abstract. Guyed towers are widely used in various engineering applications, such as telecommunications, broadcasting, and power transmission, due to their slender geometry, favorable structural performance under service loads, and economic efficiency. However, numerous structural failures resulting in tower collapse are often associated with stay cable rupture or malfunction. In this context, this study aims to investigates the nonlinear static analysis equilibrium and structural stability of a three-dimensional guyed truss tower with a height of 8 meters and a width of 1 meter, taking into account the hypothesis of unilateral contact of the guys and the deformation of the central mast. The tower has eight guy wires modeled as bar elements arranged in a fan-like configuration, anchored 1.5 meters from the central axis. To achieve this, a positional formulation combined with the Euler–Lagrange equations is employed. Using Matcont, the nonlinear system is solved to obtain equilibrium paths and assess their stability when the guyed tower is subjected to purely horizontal load. Equilibrium paths were obtained revealing complex nonlinear responses coexisting at the same load level. This indicates an abundance of stable solutions and demonstrates that dynamic perturbations around these solutions can also lead to a rich spectrum of oscillatory behaviors.

Keywords: Nonlinear static; stability; unilateral contact; Guyed tower;

1 Introduction

Guyed towers are widely used in various engineering applications, such as telecommunications, broadcasting, and power transmission, due to their slender geometry, greater height, efficient, favorable structural performance under service loads, and economic efficiency. However, numerous structural failures interrupt their operation and intended purpose, causing many accidents and collapse. Due to the various mechanisms that lead to failure in this structural system, several studies have been conducted to understand their complex structural behavior, considering both static and dynamic loading conditions.

Kahla [1] investigated the nonlinear response of a 152.4 meters three-dimensional guyed tower using a finite element model. The results showed that, during the nonlinear response, the structure failed due to compressive forces induced by the cables. Carvalho [2] and Del Prado *et al.* [3] investigated the dynamic response of imperfect guyed structures based on finite element formulations, a nonlinear discrete model, and the Budiansky criterion. They concluded that, depending on the load characteristics, the system is sensitive to imperfections and demonstrated that the post-critical behavior is strongly influenced by the guy wires. Bentes [4] identified that guyed towers exhibit a predominant torsional effect around the vertical axis of the structure. Marques *et al.* [5] investigated the influence of the cable system on the stability of guyed towers by combining analytical studies with nonlinear numerical simulations. They found that the parameters significantly affect the nonlinear response. Cucuzza *et al.* [6] analyzed the effects of geometric nonlinearities on the responses of a continuous structural model of a guyed tower. The results indicate that the studied model exhibits a highly nonlinear response, even under low load levels. According to Silva [7], greater slenderness structure are more susceptible to lateral deflections and loss of stability, structural damage and, structural collapse caused by cable rupture.

Greco [8] used the positional formulation to describes the kinematics of the elements relative to their fixed initial coordinate system used. The development of the equilibrium equations is based on the structural equilibrium from the positions of the bar element nodes, where the nodal positions or coordinates in the deformed configurations are the unknowns of the problem. Carrazedo and Coda [9] investigated thermomechanical coupling in im-

pacts between trusses and rigid obstacles and concluded that the positional formulation is accurate and efficiently captures the complex responses of tall and slender structures undergoing large deformations, displacements, and rotations. Eduardo Júnior *et al.* [10] replaced the conventional displacement parameterization to directly model the nonlinear kinematics of truss structures and capture nonlinear or large deformation behaviors, providing accuracy in structural analysis and efficiency in handling certain boundary conditions and complex behaviors.

Therefore, despite numerous studies addressing the complex responses of guyed towers, it is important to highlight that their structural analysis still faces significant challenges concerning geometric nonlinearities, simplifications related to the consideration of guy wire contact, and the analysis of structural stability.

In this context, the present work investigates the nonlinear static equilibrium and structural stability of a three-dimensional guyed truss tower, taking into account the unilateral contact hypothesis. To achieve this, a positional formulation combined with the Euler–Lagrange equations is employed to obtain a set of nonlinear ordinary differential equations that describe the structural behavior of the guyed tower. These system, is then solved to obtain equilibrium paths and assess their stability when the guyed tower is subjected to horizontal load.

2 Problem formulation

Figure 1 shows the initial configuration, with length l_0, and the current configuration, with length l, of a generic bar in an arbitrary structure, relative to a fixed reference frame with directions 1, 2, and 3. The coordinates of the two nodes of the bar in the initial and current configurations are denoted in the figure as X and Y, respectively. Superscripts refer to the bar's node index, while subscripts refer to the analyzed direction.

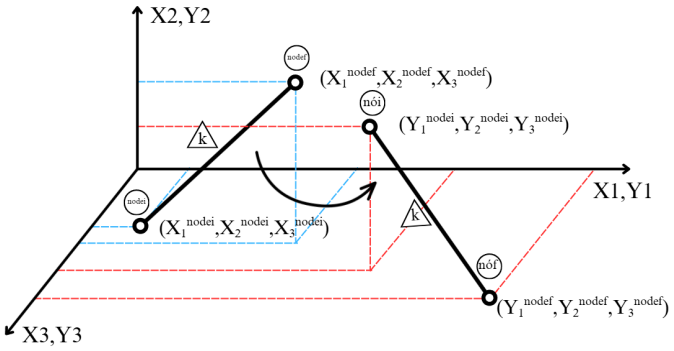


Figure 1. Member element with uniaxial stiffness and change of configuration

The energy of a structural system is described using the Lagrangian function ($\mathcal{L}$), defined as the difference between the Kinetic Energy ($\mathbb{K}$) and the Total Potential Energy (Π). The Total Potential Energy, in turn, is the sum of the Internal Strain Energy ($\mathbb{U}$) and the Potential Energy of the External Forces ($\mathbb{P}$), as presented in:

$$\mathcal{L}(Y_i^\alpha, \dot{Y}_i^\alpha, t) = \mathbb{K}(\dot{Y}_i^\alpha) - \Pi(Y_i^\alpha) = \mathbb{K}(\dot{Y}_i^\alpha) - (\mathbb{U}(Y_i^\alpha) + \mathbb{P}(Y_i^\alpha)) \tag{1}$$

The generalized variables of the Lagrangian function ($\mathcal{L}$) are the current positional coordinates of all the structure's nodes, denoted by Y_i^α, their time derivatives $\dot{Y}_i^\alpha$, representing velocities, and time t. The index α refers to the global nodes of the structure, that varies from 1 to the total number of nodes in the system, while the index i indicates the directions of the fixed reference system (directions 1, 2, and 3). As noted, the Kinetic Energy ($\mathbb{K}$) is expressed as a function of the velocities $\dot{Y}_i^\alpha$, whereas the Total Potential Energy (Π), Strain Energy ($\mathbb{U}$), and the Potential Energy of External Forces ($\mathbb{P}$) are defined as functions of the positions Y_i^α.

The Potential Energy of External Forces ($\mathbb{P}$) is obtained by multiplying the external forces by the current positions of their respective global nodes β and the directions j in which they are applied, as shown below:

$$\mathbb{P} = -F_j^\beta Y_j^\beta \tag{2}$$

The Internal Strain Energy ($\mathbb{U}$) of the structure is calculated as the sum of the Internal Strain Energy of all bar elements ($nelems$) comprising the structure, which is obtained by integrating the specific strain energy (u_e) over the initial volume of each bar element (k) of the structure:

$$\mathbb{U} = \sum_{k=1}^{nelems} \mathbb{U}_e^{(k)} \quad => \quad \mathbb{U}_e^{(k)} = \int_{V_0^{(k)}} u_e^{(k)} \, dV_0 \tag{3}$$

Adopting the Saint-Venant–Kirchhoff constitutive model, the specific strain energy ($u_e^{(k)}$) of each bar element (k) in the structure is expressed as a function of the bar's longitudinal modulus of elasticity (E) and the Green–Lagrange strain ($\mathbb{E}^{(k)}$). The Green-Lagrange strain relates the initial length ($l_0^{(k)}$) and final length ($l^{(k)}$) of the bars, as expressed by the following equations:

$$u_e^{(k)} = \frac{1}{2} E^{(k)} \mathbb{E}^{(k)^2} \quad ; \quad \mathbb{E}^{(k)} = \frac{1}{2}\left[\left(\frac{l^{(k)}}{l_0^{(k)}}\right)^2 - 1\right] \tag{4}$$

From the node coordinates, as shown in Fig. 1, it is possible to express the initial length $l_0^{(k)}$ and the current length $l^{(k)}$ of each bar as functions of the positions, as follows:

$$l_0^{(k)} = \sqrt{(X_1^{nodef^{(k)}} - X_1^{nodei^{(k)}})^2 + (X_2^{nodef^{(k)}} - X_2^{nodei^{(k)}})^2 + (X_3^{nodef^{(k)}} - X_3^{nodei^{(k)}})^2} \tag{5}$$

$$l^{(k)} = \sqrt{(Y_1^{nodef^{(k)}} - Y_1^{nodei^{(k)}})^2 + (Y_2^{nodef^{(k)}} - Y_2^{nodei^{(k)}})^2 + (Y_3^{nodef^{(k)}} - Y_3^{nodei^{(k)}})^2} \tag{6}$$

Assuming that the mass ($M^{(k)}$) of each bar element (k) is concentrated at the structure's nodes. The mass at a node should account for the masses of all bars connected to that node. The Total Kinetic Energy ($\mathbb{K}$) of the system is then given by:

$$\mathbb{K} = \sum_{k=1}^{nelems} \frac{1}{2} M^{(k)} \dot{Y}_i^{\alpha} \dot{Y}_i^{\alpha} \tag{7}$$

The equilibrium equations, that comprise the system of equilibrium equations, are derived using the eqs. (2), (3) and (7), with the following Euler-Lagrange equations:

$$-\frac{\partial \mathbb{U}}{\partial Y_i^{\alpha}} - \frac{\partial \mathbb{P}}{\partial Y_i^{\alpha}} - \frac{d}{dt}\left(\frac{\partial \mathbb{K}}{\partial \dot{Y}_i^{\alpha}}\right) = F_i^{\alpha\ (amort)} \tag{8}$$

Expanding the eq. (8), the first term, derived from the internal strain energy with respect to the positions, corresponds to the internal force ($F_i^{(\mathrm{int})}$). Applying the chain rule to the derivative of the specific strain energy denotes $u_e^{(k)}$, and noting that the energy conjugate of the Green–Lagrange strain is the second Piola–Kirchhoff stress tensor ($\mathbb{S}$), which, based on eq. (3), can be written as:

$$F_i^{\alpha\ (int)} = \sum_{k=1}^{nelems} \mathbb{S}^{(k)} \frac{(-1)^{\gamma^{(k)}}}{l_0^{(k)^2}} (Y_j^{\mathrm{nó}f^{(k)}} - Y_j^{\mathrm{nó}i^{(k)}}) \delta_{\alpha\gamma^{(k)}} \delta_{ij} \tag{9}$$

where the Kronecker deltas $\delta_{\alpha\gamma^{(k)}}$ and δ_{ij} are applied to the equation to ensure that components of the derivative of the Green-Lagrange deformation contribute to the vector of internal forces only at positions where the nodes and the local and global directions coincide. To properly analyze the interaction between the central mast and the stay cables taking account the assumption of unilateral contact of the stays, the determination of the internal force is divided into two components: the first summation of eq. (10) refers to the internal forces originating from the bar elements of the tower mast, while the second summation of eq. (10) corresponds to the internal forces generated by the stays. Therefore, the total number of elements in the system, denoted as $nelems$, results from the sum of the number of bars and the number of stays, that is, $nelems = nbars + nguys$. Accordingly, the internal force is rewritten as:

$$\begin{aligned} F_i^{\alpha\ (int)} = & \sum_{k=1}^{nbars} \mathbb{S}^{(k)} \frac{(-1)^{\gamma^{(k)}}}{l_0^{(k)^2}} (Y_j^{2^{(k)}} - Y_j^{1^{(k)}}) \delta_{\alpha\gamma^{(k)}} \delta_{ij} \\ & + \sum_{k=1}^{nguys} \mathbb{S}^{(k)} \frac{(-1)^{\gamma^{(k)}}}{l_0^{(k)^2}} (Y_j^{2^{(k)}} - Y_j^{1^{(k)}}) \delta_{\alpha\gamma^{(k)}} \delta_{ij} FS^{(k)} \end{aligned} \tag{10}$$

Also in the eq. (10), the term $FS^{(k)}$ represents a signum-type function that incorporates the displacement dependency of the elements for determining the final internal force in the stay cables. This term is given by:

$$FS^{(k)} = \left(\frac{1}{2} + \frac{signum(l^{(k)} - l_0^{(k)})}{2}\right) \tag{11}$$

Returning to eq. (8), the derivative of term of the Potential Energy of the External Forces with respect to the positions results in the vector of external forces ($F_i^{\alpha\ (ext)}$) of the structure which is defined as:

$$F_i^{\alpha\ (ext)} = \frac{\partial \mathbb{P}}{\partial Y_i^\alpha} = -\frac{\partial}{\partial Y_i^\alpha}(F_j^\beta Y_j^\beta) = -F_j^\beta \delta_{\alpha\beta}\delta_{ij} \tag{12}$$

The development of the last part of the Euler-Lagrange equations (8), which involves the Kinetic Energy of the system of the equation, results in the Inertial Force ($F_i^{\alpha\ (iner)}$) of the system described as:

$$F_i^{\alpha\ (iner)} = \frac{d}{dt}\left(\frac{\partial \mathbb{K}}{\partial \dot{Y}_i^\alpha}\right) = \sum_{k=1}^{nelems} \frac{d}{dt}(M^{(k)}\dot{Y}_i^\alpha) = \sum_{k=1}^{nelems} M^{(k)}\ddot{Y}_i^\alpha \tag{13}$$

The structural damping was incorporated into the equations of motion of the structure by operating the product between the matrix $\mathbf{C}^{(k)}$ and the vector of nodal velocities $\dot{Y}_i^\alpha$, as shown in:

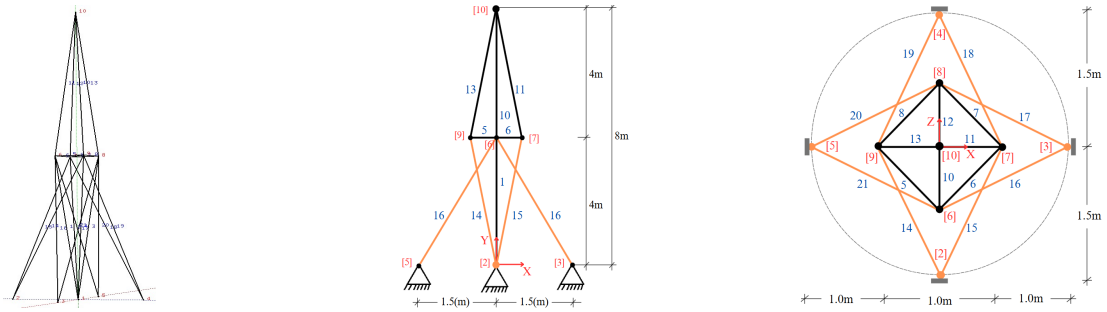
$$F_i^{\alpha\ (amort)} = -\sum_{k=1}^{nelems} \mathbf{C^{(k)}}\,\dot{Y}_i^\alpha \tag{14}$$

So, the general equation of motion for a structural system considering all degrees of freedom is given by:

$$F_i^{\alpha\ (iner)} + F_i^{\alpha\ (amort)} + F_i^{\alpha\ (int)} = F_i^{\alpha\ (ext)} \tag{15}$$

3 Numerical results

The discrete model of the guyed tower used in this work is shown in Fig. 2. It consists of a central mast formed by a truss measuring 8 m in height and 1 m in width, composed by 21 elements interconnected at ten nodes. The central mast is supported at a single node, referred to as node 1, which serves as the main base support for the entire structure. Nodes 2, 3, 4, and 5 are fixed anchoring points for the guy wires, spaced 1.5 m from the origin point (node 1). The stability is enhanced by eight guy wires. Each anchoring point, nodes 2, 3, 4, and 5, supports two guy wires, which are connected at their upper ends to intermediate nodes 6, 7, 8, and 9, located 4 m above the base of the central mast, and spaced 0.5 m from the origin point (node 1). Each of these intermediate nodes also receives two guy wires, as illustrated in Fig. 2.



(a) (b) (c)

Figure 2. Discrete model of the guyed tower in (a) perspective, (b) front view and (c) plan view.

The interaction between the central mast and the guy wires is accounted for by establishing the attachments and constraints at the anchoring nodes and connection points along the mast's height and exhibiting stiffness only when in tension.

The solution of the nonlinear equilibrium equation system (Eq. 15) is performed via numerical continuation methods implemented in the MatCont, an continuation package, version 7.5, based on the arc-length criterion, implemented in conjunction with a Newton–Raphson or Newton–Krylov method adapted for arc-length continuation. Using Floquet multipliers, all system's equilibrium paths are analyzed and the stability was evaluated.

The bars comprising the central mast and the guy wires are made of steel with an Young Modulus of $E = 2 \cdot 10^8$ kN/m^2, a density of $\rho = 7850$ kg/m^3, and a cross-sectional area of $A = 785 \cdot 10^{-3}$ m^2. In this study, a viscous damping coefficient proportional to mass, $\boldsymbol{c}$, is assumed equal to 1%.

The nonlinear equilibrium paths of the guyed tower, showed in Fig. 2, are evaluated in two principal cases. The first one, assesses the behavior of the guyed tower under purely horizontal loading with the assumption of

bilateral contact hypothesis, where the stays are modeled as bar elements, possessing inherent stiffness in both compression and tension. For that, $FS^{(k)}$ in eq. (10) is assumed equal to one. The second case examines the guyed tower when it is also subjected by purely horizontal loading and the stays are modeled according to the unilateral contact hypothesis. This assumption implies that the stays exhibit stiffness only when they are in tension.

Figure 3 depicts the nonlinear static equilibrium paths of the stayed tower, when it is subjected to a purely horizontal load $P_1^{10} \times 10^8$ (N), applied in the X direction Y_1^{10}. In this figure, the stays contact are defined as bilateral. The equilibrium paths are projected onto the planes (a) P_1^{10}-Y_1^{10}, (b) P_1^{10}-Y_3^{10} and (c) P_1^{10}-Y_2^{10}, that illustrate displacements along the X-axis, Z-axis, and Y-axis directions, respectively. It is observed from Figs. 3a and 3b that they display the antisymmetric and analogous nonlinear equilibrium trajectories, in relation to the initial configuration of the guyed tower, for the displacements in the X-axis and Z-axis directions, respectively. The tower exhibits several extended, well defined stable equilibrium paths, highlighted in blue. These figures also present multiple unstable equilibrium trajectories, highlighted in red, which indicate the critical load thresholds beyond which lateral stability is lost, thereby revealing the existence of multiple equilibrium configurations corresponding to the same load magnitude.

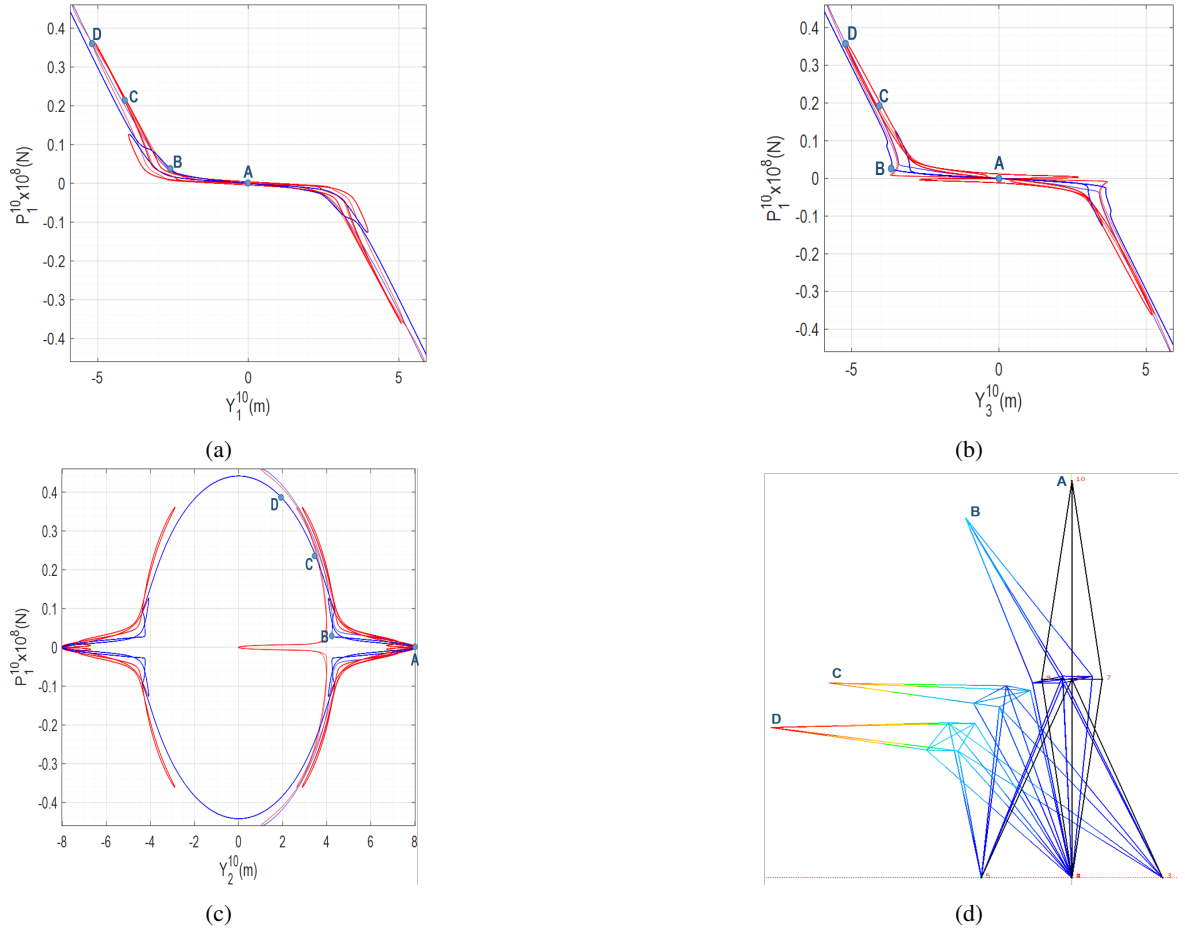


Figure 3. Nonlinear static equilibrium path of the stayed tower under horizontal loading at the top node in the direction X. Bilateral contact hypothesis. Projection onto the planes (a) $P_1^{10} - Y_1^{10}$, (b) $P_1^{10} - Y_3^{10}$ and (c) $P_1^{10} - Y_2^{10}$, (d) Displaced configuration.

The resulting horizontal displacements in directions Y_1^{10} and Y_3^{10}, Figs. 3a and 3b, range approximately from $[-5.9, 5.9]m$ under a load variation on the order of $\pm 0.5 \times 10^8$ N. From these responses, can also identify points where transitions between equilibrium states occur smoothly, indicating changes in the stayed-tower's equilibrium configuration. Additionally, there are regions susceptible to phenomena such as snap-through or snap-back, signifying abrupt stability loss. It is noteworthy that the similarity in response patterns observed in Y_1^{10} and Y_3^{10} directions, both in displacement magnitude and applied load, demonstrates that the global stiffness of the stayed tower in the $X-$ and $Z-$axis directions is equivalent. On the other hand, their similarity implies directional coupling between $X-$ and $Z-$displacements due to the load variation, influencing behavior in both directions that is an indicator of geometric instability, accompanied by the twisting of the central mast. When examining the range between $[-2, 2]m$, it becomes evident that the tower exhibits larger displacements around the zero load

condition, suggesting low global stiffness. However, both stable and unstable equilibrium paths run parallel and sometimes overlap, reflecting a deformation of central mast. As the applied load increases, the tower's global stiffness rises, reducing and constraining displacements. Within this regime, an abrupt transition occurs, indicating a redistribution of the internal forces and reconfiguration of the structural equilibrium.

Analyzing Fig. 3c in relation to the vertical displacements, the stayed tower exhibits symmetrical equilibrium curves. The structure demonstrates a prolonged stable equilibrium path, along with several unstable equilibrium trajectories. Maximum vertical displacements reach approximately from $[-8, 8]m$ under a load variation between $\pm 0.5 \times 10^8$ N. Based on the static nonlinear response analysis, these symmetric equilibrium branches reflect the geometric stability characteristics inherent to the tower's reconfigured structure. Otherwise, multiple coexisting stable and unstable equilibrium branches are observed in the equilibrium path when the tower displaces approximately $8m$ (inverted mast) from its initial position. Small load variations in these branches can trigger snap-through or snap-back behavior, lead to larger displacements of tower. Figure 3d illustrates the displaced configurations of the stayed tower in the chosen points $(A - D)$ of the nonlinear equilibrium path, showing the variability in displacement amplitude along this curve.

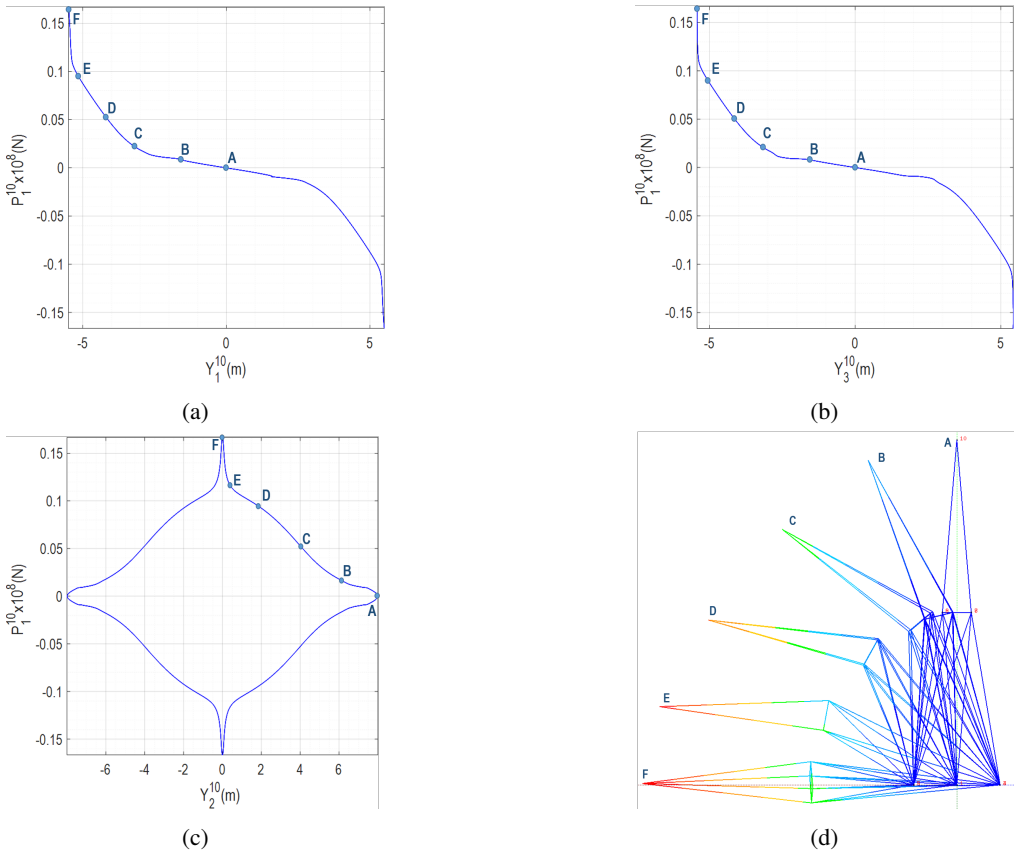


Figure 4. Nonlinear static equilibrium path of the stayed tower under horizontal loading at the top node in the direction X. Unilateral contact hypothesis. Projection onto the planes (a) $P_1^{10} - Y_1^{10}$, (b) $P_1^{10} - Y_3^{10}$ and (c) $P_1^{10} - Y_2^{10}$, (d) Displaced configuration.

Figure 4 presents nonlinear equilibrium trajectories of the stayed tower under horizontal loading applied in the X-Axis direction at top node 10, according unilateral contact hypothesis of the stays. Nonetheless, considering the equilibrium response in the projections $P_1^{10} - Y_1^{10}$ and $P_1^{10} - Y_3^{10}$, Figs. 4a and 4b, respectively, it is possible to observe that for the same loading variations the tower display the antisymmetric, in relation to the initial configuration of the tower, analogous and stable nonlinear equilibrium paths that is highlighted in blue. The maximum horizontal displacements in the X- axis and $Z-$Axis directions is around of ± 5.5 (m), for horizontal loading variation of approximately $\pm 0.2 \times 10^8$ N. This indicates that the unilateral contact of the stay cables affects strongly the stability of the tower and reduces the range of the applied horizontal load.

Figure 4c display the symmetric nonlinear equilibrium path in the vertical direction Y_2^{10}, of the stayed tower in the projection, $P_1^{10} - Y_2^{10}$, $Y-$Axis direction, when it's applied horizontal loading in the X direction. The maximum horizontal displacements of guyed tower in this direction is around of $\pm 8\ m$ for applied loading about $\pm 0.2 \times 10^8$ N. The analysis demonstrates that, under horizontal load in the X direction, the tower exhibits

stable nonlinear equilibrium path that indicate large displacments of the tower, leading the tower to its inverted configuration without a snap-through phenomena. It is important highlight that these equilibrium paths indicates a cyclic dependence of the structural response to load variations. Figure 4d presents chosen displaced configuration of the guyed tower, points $(A - F)$ of nonlinear equilibrium path, to highlight the large displacements observed in the tower.

4 Conclusions

This work investigated the nonlinear static equilibrium and structural stability of a three-dimensional guyed truss tower under horizontal load, taking into account the bilateral and unilateral contact hypothesis of the guys. To achieve this, a positional formulation combined with the Euler–Lagrange equations was employed to obtain a set of nonlinear ordinary differential equations that describe the structural behavior of the guyed tower. The horizontal loading in the $X-$direction induced a complex nonlinear static behavior with sudden changes in the equilibrium configuration relative to the tower's initial position, accompanied by significant vertical displacements in comparison to horizontal ones. For the same loading applied in the guyed tower, this work revealed that the stiffness of the tower with unilateral contact assumption of the guys was lower compared to the stiffness observed when the guyed tower was analyzed with the bilateral contact assumption. In this case, the maximum horizontal load was less than the bilateral case. On the other hand, the unilateral case eliminated the unstable paths of the nonlinear equilibrium path, creating a unique stable configuration of the guyed tower.

Acknowledgements. The authors are grateful for the financial support provided by CAPES, CNPq and FAPEG for the development of this work.

Authorship statement. The authors hereby confirm that they are the sole liable persons responsible for the authorship of this work, and that all material that has been herein included as part of the present paper is either the property (and authorship) of the authors, or has the permission of the owners to be included here.

References

[1] N. BEN KAHLA. Nonlinear dynamic response of a guyed tower to a sudden guy rupture. *Engineering Structures*, vol. 19, n. 11, pp. 879–890, 1997.
[2] E. C. CARVALHO. Análise da instabilidade dinâmica de estruturas estaiadas. Dissertação (mestrado), Universidade Federal de Goiás, Escola de Engenharia Civil, Goiânia, GO, 2008.
[3] Z. J. G. N. DEL PRADO, E. C. CARVALHO, and P. B. GONCALVES. Dynamic stability of imperfect cable stayed masts. *Mecánica Computacional*, vol. 24, n. 7, pp. 647–658, 2010.
[4] J. L. BENTES. Análise dinâmica da ruptura de cabos em torres autoportantes e estaiadas de linhas de transmissão. Dissertação de mestrado, Universidade Federal do Rio Grande do Sul, Porto Alegre, Brasil, 2013.
[5] R. MARQUES, P. B. GONÇALVES, and D. M. ROEHL. Effect of the cable system on the static and dynamic stability of guyed towers. In *Proceedings of the International Congress of Computational Methods in Engineering and Sciences and III Pan-American Congress on Computational Mechanics (CILAMCE–PANACM)*, Rio de Janeiro, Brazil, 2021.
[6] R. CUCUZZA, M. M. ROSSO, A. ALOISIO, J. MELCHIORRE, M. L. GIUDICE, and G. C. MARANO. Size and shape optimization of a guyed mast structure under wind, ice and seismic loading. *Applied Sciences*, vol. 12, n. 10, pp. 4875, 2022.
[7] F. N. D. SILVA. Modelo mecânico discreto para análise dinâmica não linear de torres estaiadas planas considerando o contato unilateral dos estais. Dissertação de mestrado, Universidade Federal de Goiás, Goiânia, Brasil, 2023.
[8] M. GRECO, I. P. FERREIRA, and F. B. BARROS. A classical time integration method applied for solution of nonlinear equations of a double-layer tensegrity. *Journal of the Brazilian Society of Mechanical Sciences and Engineering*, vol. 35, pp. 41–50, 2013.
[9] F. CARRAZEDO and A. CODA. Thermo-mechanical coupling in impact problems between trusses and a rigid obstacle using the positional finite element method. *Journal of Impact Engineering*, vol. 37, n. 2, pp. 320–330, 2010.
[10] A. V. EDUARDO JÚNIOR, A. D. A. ALBUQUERQUE, and D. D. L. ARAÚJO. Geometrically nonlinear analysis of planar frame structures with positional finite element method. In *XLV Ibero-Latin American Congress on Computational Methods in Engineering (CILAMCE)*, pp. 1–12, 2024.